

Hollow organic polymeric nano-bowls-supported BINOL-derived chiral phosphoric acid: enhanced catalytic performances in the enantioselective allylation of aromatic aldehydes



Zhengwei Yan, Guangxin Xie, Jianing Zhang, Xuebing Ma*

Key Laboratory of Applied Chemistry of Chongqing Municipality, College of Chemistry and Chemical Engineering, Southwest University, Chongqing, 400715, PR China

ARTICLE INFO

Keywords:

Heterogeneous organocatalysis
Chiral phosphoric acid
Enhanced catalytic performance
Hollow nano-bowl
Allylation

ABSTRACT

To improve the catalytic efficiency of expensive and versatile 1, 1'-binaphthol-derived chiral phosphoric acid with 2, 4, 6-tris(isopropyl)phenyl substituents and mass transfer of reactants in heterogeneous catalysis, a hollow organic polymeric nano-bowl was used as an effective catalyst support to anchor chiral phosphoric acid through the copolymerization of vinylated 1, 1'-binaphthol with 2, 4, 6-tris(isopropyl)phenyl substituents with styrene on the surface of polystyrene nanosphere core, etching polystyrene nanosphere by DMF and then phosphorylation by POCl₃. From the comparative kinetic investigation on the reaction rate of reactant in the asymmetric allylboration of 4-chlorobenzaldehyde with allylboronic pinacol ester, the as-fabricated hollow organic polymeric nano-bowl-supported chiral phosphoric acid displayed higher catalytic rates than ever-reported similar catalyst and possessed a constant catalytic rate (0.031 mol L⁻¹ h⁻¹) during the whole process. The expanded scope of aromatic aldehydes further proved that the hollow organic polymeric nano-bowl-supported chiral phosphoric acid was more highly active and enantioselective owing to its thin shell thickness (18 nm) and hollow structure. Due to the constant phosphorus content and well-shaped morphology of the 6th-reused catalyst, the yield of (R)-1-phenylbut-3-en-1-ol (95%) with a slightly lowered enantioselectivity (94% ee) remained constant in the sixth run. Moreover, the lowered enantioselectivity of the 6th-reused catalyst could be restored by hydrochloric acid to achieve its original enantioselectivity (96% ee), and the prothetic hollow organic polymeric nano-bowl-supported chiral phosphoric acid could effectively promote the asymmetric allylboration reaction in high yields (92–95%) with excellent enantioselectivities (94–96% ee) for another six cycles.

1. Introduction

The driving force for the development of heterogeneous enantioselective metal catalyst and organocatalyst stemmed from the practical advantages they might offer over their homogeneous counterparts in terms of process scalability, catalyst reusability, cost and purification [1–3]. Recently, due to the spectacular synthesis of well-shaped metal catalysts, heterogeneous metal catalysis paid special attention to the morphology-dependant catalytic performance of metal catalysts [4,5]. Although the well-controlled construction of organic polymer-supported organocatalyst was still in its infancy, the clues in enhanced catalytic activity had also gradually drawn more attentions [6].

1, 1'-binaphthol (BINOL)-derived chiral phosphoric acid with the 2, 4, 6-tris(isopropyl)phenyl substituents in the 3, 3' positions, commonly known as TRIP [7], had proved to be the most successful and versatile

enantioselective Brønsted acid catalyst [8–12], and was widely used in the various asymmetric catalytic transformations such as transfer hydrogenation [13–17], cycloaddition [18–20], cascade multi-component reaction [21–23], rearrangement [24,25], Mannich reaction [26], hydroxyalkylation [27], desymmetrization [28], Friedel-Crafts reactions [29–31] and miscellaneous cyclizations [32,33]. However, versatile TRIP presented a main disadvantage of long and tedious reaction sequences required for its preparation from chiral BINOL, resulting in the extremely high cost of TRIP in large-scale application. From the perspective of large-scale application, achieving the sustainability and efficiency of TRIP could significantly reduce its high cost, although additional modifications were needed. One strategy was the immobilization of TRIP onto solid support to effectively reduce its high cost owing to the recovery and reuse of TRIP [34–38]. Among them, polystyrene-supported TRIP (PS-TRIP) was used as a famous abundantly recyclable catalyst for the highly enantioselective allylboration

* Corresponding author.

E-mail address: zcj123@swu.edu.cn (X. Ma).

<https://doi.org/10.1016/j.mcat.2018.12.014>

Received 21 October 2018; Received in revised form 17 December 2018; Accepted 18 December 2018

Available online 28 December 2018

2468-8231/ © 2018 Elsevier B.V. All rights reserved.

of aldehydes in batch and flow [36]. Another strategy was the further enhancement of catalytic efficiency of supported TRIP by improving the accessibility of reactants to the catalytic sites of TRIP. However, to the best of our knowledge, no attention was paid on the further improvement in mass transfer of reactants and effectiveness factor (η) of anchored TRIP.

The enhancement of mass transfer of reactants to active catalytic sites had always been one of the most consistently pursued research topics in the field of heterogeneous catalysis. Owing to hollow interior and well-shaped morphology, hollow nanospheres displayed the exquisite advantages such as large specific surface area and pore volume, high loading capacity of catalyst and internal/external concentration difference in heterogeneous catalysis [39,40]. Recently, the hollow structures [41–44] and well-shaped nanosphere [45] in the improved mass transfer of reactants and products into and out catalyst backbone in heterogeneous organocatalysis were highlighted. In this paper, to take advantage of the merits of hollow structure and thin shell thickness, hollow organic polymeric nano-bowls-supported BINOL-derived chiral phosphoric acid (HOPBs-TRIP) was fabricated for the first time via the first copolymerization of (R)-6 with styrene on the surface of poly(styrene/acrylic acid) nanosphere (PS), subsequent etching PS by DMF and final functionalization by POCl₃ (Scheme 1). Due to the effective improvement in the mass transfer of reactants resulted from hollow structure and thin shell thickness (18 nm), the as-fabricated HOPBs-TRIP displayed higher catalytic performances including activities and enantioselectivities than ever-reported PS-TRIP in the heterogeneous enantioselective allylation of aldehydes [36] and showed better economical efficiency than homogeneous TRIP.

2. Experimental

2.1. Materials and sample characterization

Styrene (St) was purified by distillation under reduced pressure before use. Styryl-derived monomer (R)-6 and poly(styrene/acrylic acid) nanospheres (PS) (327 ± 15 nm, $n = 50$) were synthesized according to the procedures shown in ESI†. The other chemicals were of analytical grade and used as received from commercial suppliers without any further purification.

¹H and ¹³C NMR spectra were conducted on a Bruker av-600 NMR instrument, in which all chemical shifts were reported down-field in

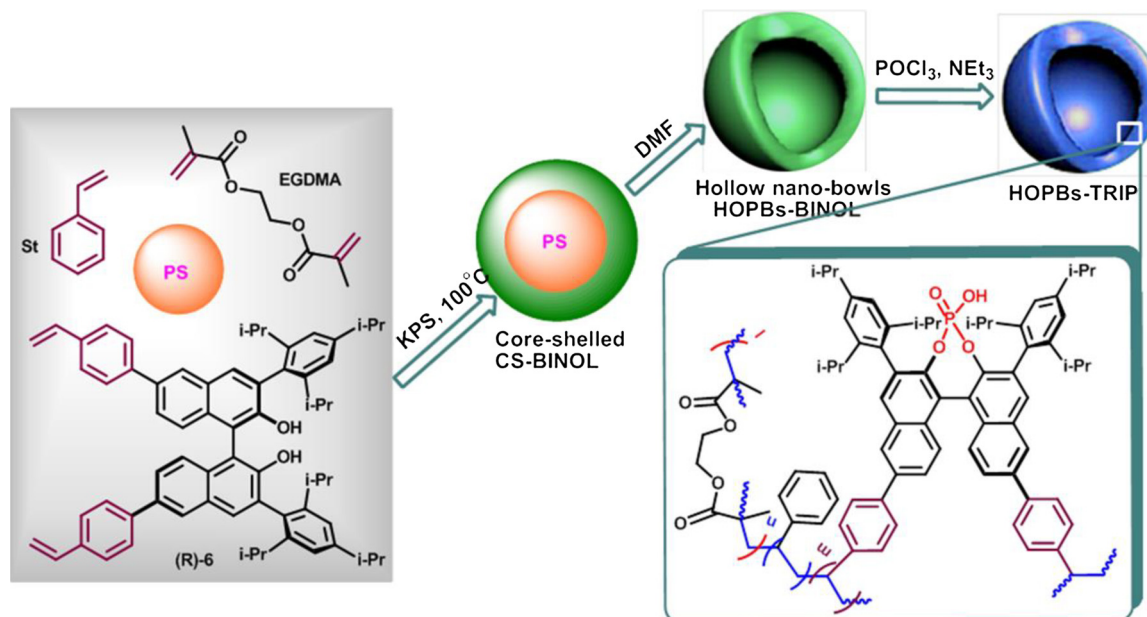
ppm relative to the hydrogen and carbon resonances of TMS. The loading capacity of phosphoric acid was determined by ICP-OES/ICP-MS Agilent 725 after the sample was digested. The morphology was observed by JEM-2100F scanning electron microscopy and S-4800 transmission electron microscope, respectively operated at 10 kV and 200 kV. FT-IR spectroscopy was performed on a Perkin-Elmer model GX spectrometer using the KBr pellet. The enantiomeric excesses (% ee) of products were determined by Agilent LC-1200 HPLC with a UV-vis detector on Daicel Chiralpak chiral column using heptane/isopropanol as the eluents.

2.2. General preparation of hollow organic polymeric nano-bowls-supported HOPBs-BINOL

After PS core (800 mg) was well-dispersed under magnetic stirring for 12 h at room temperature in the mixed solvents of DMSO (21 mL) and DI water (7 mL) containing polyvinyl alcohol (PVA, 0.5 wt%), a DMSO solution (4 mL) of styrene (208 mg, 2.0 mmol), (R)-6 (270 mg, 0.3 mmol) and ethylene glycol dimethyl acrylate (EGDMA, 320 mg, 1.6 mmol) was injected by syringe and irradiated by ultrasound for 30 min. The translucent emulsion was added 3 mL of aqueous potassium persulfate (KPS, 60 mg, 0.45 mmol), heated to 100 °C and stirred for 48 h. Then 9 mL of the resulting emulsion was sampled, added 1 mL of ethanol and isolated by centrifugal separation. The combined solids (CS-BINOL) were dispersed in DMF (10 mL), irradiated by ultrasound for 30 min and stirred for 3 h to remove PS core. The isolated solid was repeatedly dealt with DMF twice, washed with ethanol (10 mL × 3) and dried naturally at room temperature to afford hollow organic polymeric nano-bowls-supported HOPBs-BINOL (423 mg) as a slightly yellow solid.

2.3. Preparation of hollow organic polymeric nano-bowls-supported chiral phosphoric acid (HOPBs-TRIP)

In a dried Schlenk tube (25 mL), HOPBs-BINOL (300 mg) was suspended in a solution (5 mL) of dioxane containing triethylamine (3.0 μL, 4.0 × 10⁻³ mmol) under Ar for 0.5 h. Then, POCl₃ (18 μL, 2.0 × 10⁻³ mmol) was added, and the reaction mixture was heated to 75 °C and stirred for 14 h. The resulting reaction mixture was added THF (1 mL) and HCl solution (1 mol L⁻¹, 1.5 mL) at room temperature, heated to 50 °C, stirred for 15 h and diluted by ethanol (7 mL). The solid



Scheme 1. Preparation route to hollow organic polymeric nano-bowls-supported BINOL-derived chiral phosphoric acid (HOPBs-TRIP).

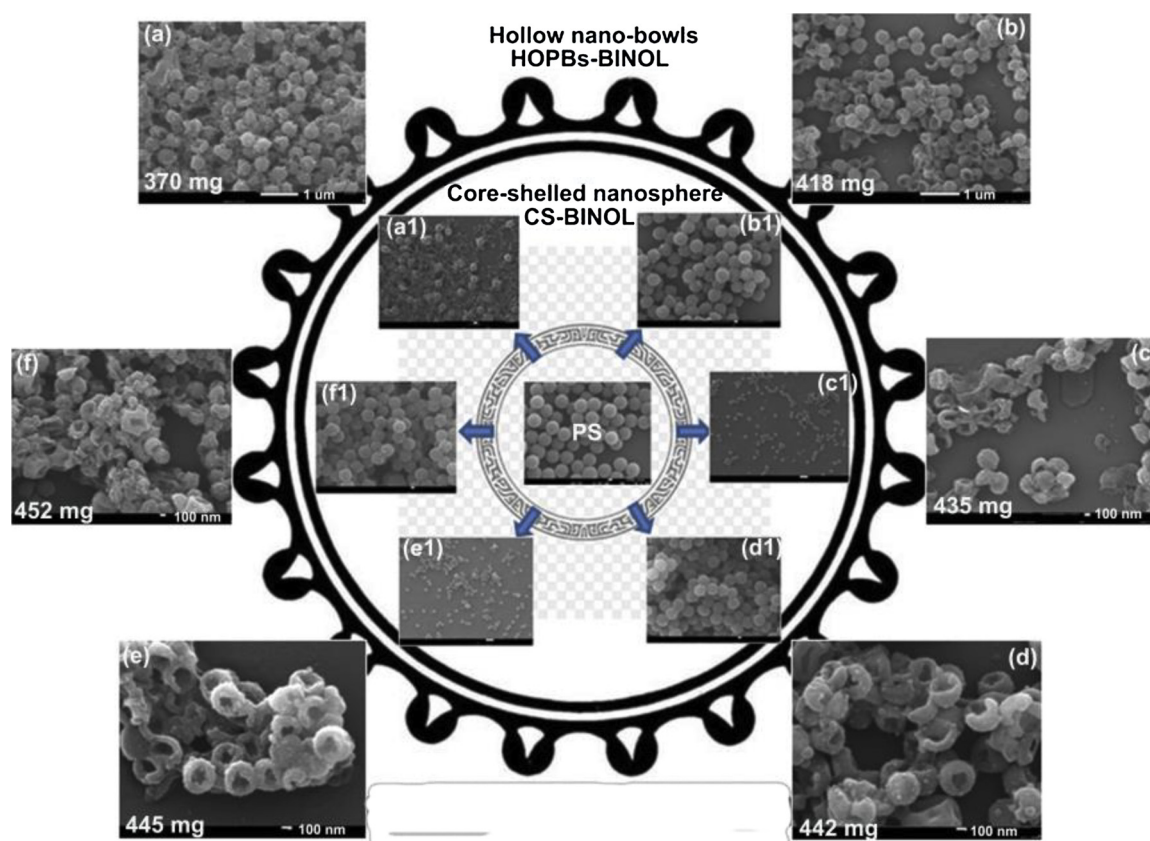


Fig. 1. SEM images of core-shelled CS-BINOL (a₁–f₁) and hollow nano-bowls-supported HOPBs-BINOL (a–f) under preparation conditions: (a₁) 500 mg PS, 24 h, 40 mg KPS; (b₁) 800 mg PS, 24 h, 40 mg KPS; (c₁) 800 mg PS, 48 h, 40 mg KPS; (d₁) 800 mg PS, 72 h, 40 mg KPS; (e₁) 800 mg PS, 48 h, 60 mg KPS; (f₁) 800 mg PS, 72 h, 80 mg KPS.

was isolated by centrifugal separation, washed with ethanol (10 mL × 3) and dried naturally at room temperature to give brown HOPBs-TRIP (303 mg).

2.4. General procedure for heterogeneous enantioselective allylation of aromatic aldehydes

A screw-cap reaction tube containing HOPBs-TRIP (66.7 mg, 5 mol %) was evacuated, flushed with Ar and charged with freshly distilled benzaldehyde (21.2 mg, 0.2 mmol) in toluene (1.0 mL). The reaction mixture was cooled to $-30\text{ }^{\circ}\text{C}$, followed by the addition of allylboronic acid pinacol ester (36.9 mg, 0.22 mmol) dropwise and stirred for 6 h. HOPBs-TRIP was recovered by centrifugal separation and directly reused in the following catalytic cycles. The centrifugate was loaded on a silica gel column and purified by flash chromatography using PE/EA ($v/v = 10:1$) to afford (*R*)-1-phenylbut-3-en-1-ol (28.1 mg, 95%) with 96% ee as a colorless oil.

3. Results and discussion

3.1. Morphological control of HOPBs-TRIP

The EGDMA-cross-linked copolymerization of styryl-attached (*R*)-6 and styrene on the surface of PS core to successfully prepare well-shaped spherical CS-BINOL was the most important and committed step. According to the ever-reported investigation [42], the emulsification of organic monomers together with PS in aqueous DMSO solution had two emulsion models—desired monomers around PS core and adverse monomers without PS core. First, we set about preparing CS-BINOL under the preliminary conditions: acrylamide (AA, 0.6 mmol), EGDMA (1.6 mmol), St (2.0 mmol), (*R*)-6 (0.17 mmol), 500 mg PS and

40 mg KPS in 35 mL of DMSO/H₂O ($v/v = 2.5$) mixed solvents for 24 h. As expected, two types of solid spheres, CS-BINOL (300–400 nm) and nanospheres (20–40 nm) with different sizes, were observed from the SEM image (Fig. 1a₁), which were resulted from the copolymerization under the control of PS and out of control of PS through different emulsion models, respectively. Subsequently, by means of weight gain of PS from 500 mg to 800 mg, the number of solid nanospheres (20–40 nm) dropped to a large extent (Fig. 1b₁) and the yield of PS-templated HOPBs-BINOL increased from 370 mg to 418 mg (Fig. 1b), which elucidated that the increased PS core strengthened the adsorption area and could effectively prevent the out of control generation of self-polymeric nanospheres. Furthermore, the enhanced coating of monomers on the surface of PS core was achieved by prolonging reaction time (24 h → 48 h → 72 h) and increasing the dosage of initiator KPS (40 mg → 80 mg), which was verified by the increased yields (418 mg → 435 mg → 452 mg) of PS-templated HOPBs-BINOL (Fig. 1c–f) and the thicker outer shell thicknesses of CS-BINOL (22 nm → 28 nm → 32 nm, Fig. S2).

According to the following relationship of effectiveness factor (η) and sphere radius (R) of catalyst in heterogenous catalysis [46,47], the more effective diffusion coefficient (D_e) and shorter sphere radius (R) are favorable for achieving a better effectiveness factor (η).

$$\eta = \frac{3}{\phi_s} \left(\frac{1}{\tanh \phi_s} - \frac{1}{\phi_s} \right) \quad (1)$$

$$\phi_s = R \sqrt{\frac{k_1}{D_e}} \quad (2)$$

where ϕ_s is Thiele modulus for sphere, k_1 is first-order kinetic constant (s^{-1}), R is sphere radius (cm) and D_e is effective diffusion coefficient ($\text{cm}^2 \text{ s}^{-1}$). To achieve the shorter transmission distance (R) of reactants

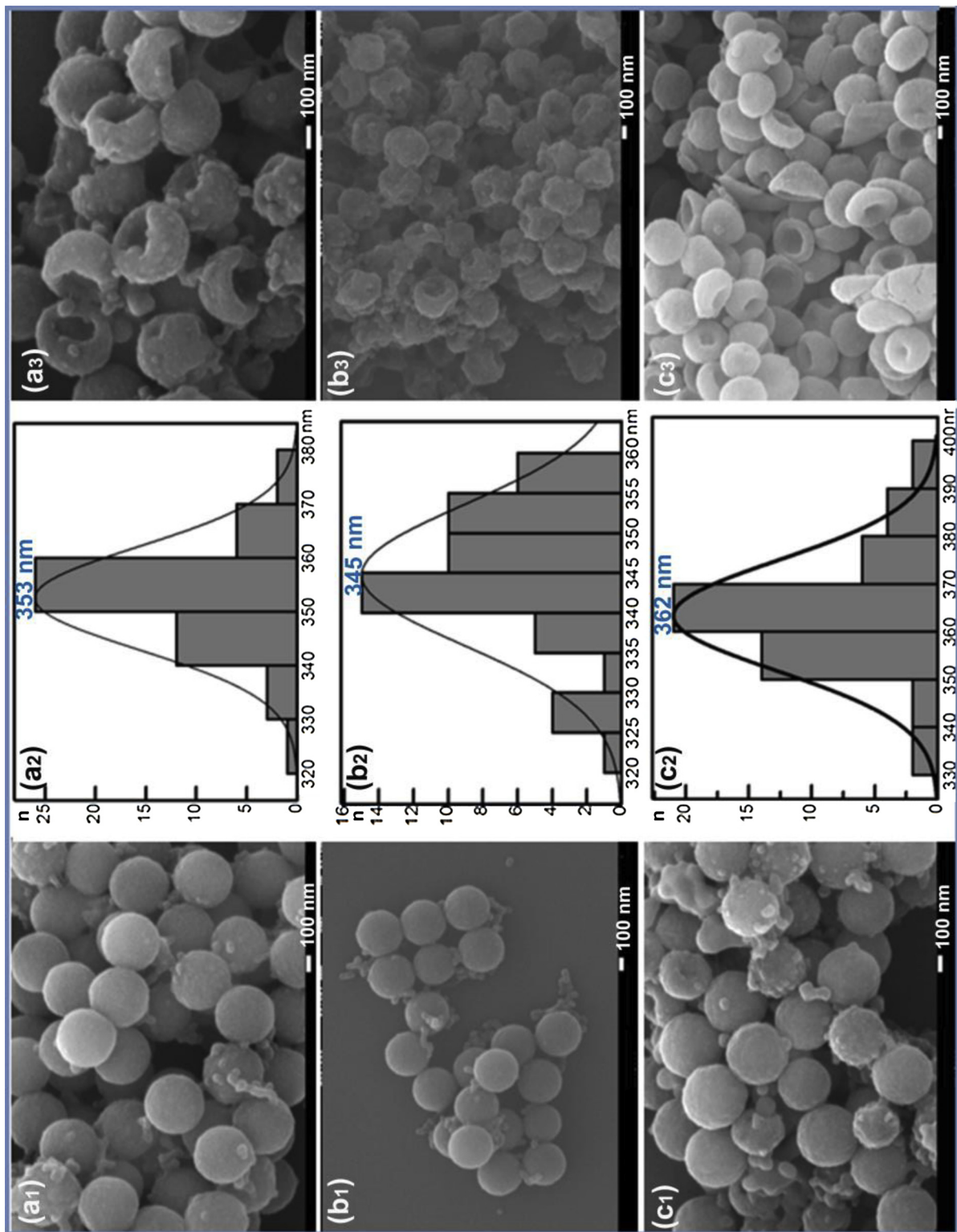


Fig. 2. SEM images (a₁–c₁), particle size distributions (a₂–c₂) of CS-BINOL and SEM images (a₃–c₃) of HOPBs-BINOL prepared under different the dosages of AA and EGDMA: (a₁) no AA, EGDMA (320 mg, 1.6 mmol); (b₁) no AA, EGDMA (160 mg, 0.8 mmol) and (c₁) no AA, EGDMA (270 mg, 0.3 mmol), (R)-6 (270 mg, 0.3 mmol).

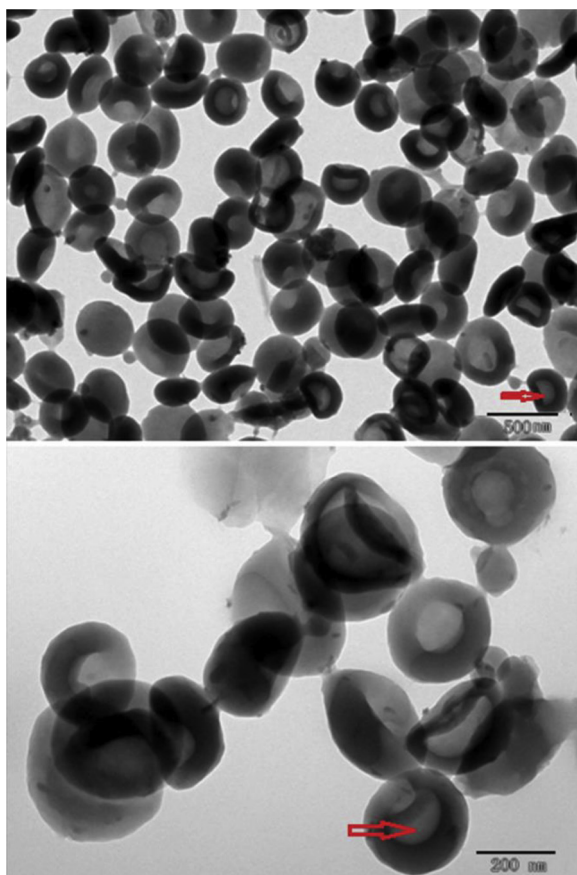


Fig. 3. TEM images of hollow organic polymeric nano-bowls HOPBs-BINOL with a kippah structure.

through heterogeneous catalyst, the shell thickness of HOPBs-BINOL was further optimized by tuning the dosages of AA and EGDMA under the following parameters (St: 2.0 mmol, (*R*)-6: 0.17 mmol, PS: 800 mg, AA: 0.6 mmol, EGDMA: 1.6 mmol and KPS: 60 mg at 100 °C for 48 h). When no directing agent AA was added, the average particle size of core-shelled CS-BINOL decreased from 388 nm to 353 nm and the average outer shell thickness decreased from 31 nm to 13 nm (Fig. 2a₂). Further halving the dosages of crosslinking agent EGDMA to 160 mg (0.8 mmol), the average outer shell thickness of core-shelled CS-BINOL (345 ± 25 nm, $n = 50$) was shortened to 9 nm (Fig. 2b₂). Meanwhile, it was found that the loading capacity of (*R*)-6 (0.09 mmol g⁻¹) was too low to meet the requirement of highly loaded TRIP. Therefore, the dosages of (*R*)-6 increased from 150 mg (0.17 mmol) to 270 mg (0.3 mmol) to achieve the higher loading capacity of (*R*)-6 (0.15 mmol g⁻¹), and then the average outer shell thickness of core-shelled CS-BINOL (362 ± 30 nm, $n = 50$) was thickened to 18 nm (Fig. 2c₂).

After the as-fabricated core-shelled CS-BINOL was etched with DMF to remove PS core, the shells would withstand the actions of osmotic pressure (P) of escaped DMF and centrifugal force (F_c). It is well-known that the pressure difference between the center and the edge of the container of radius (r) in centrifugal process is $\Delta P = \rho \omega^2 r^2 / 2$, where ρ (kg m⁻³) is the density of the fluid and ω (rad/s) is the angular velocity. Then, the pressure which acted on the shell of HOPBs-BINOL was calculated to be 2.18×10^{-8} N um⁻² in DMF (945 Kg m⁻³) at a rotation speed $\omega = 8100/60 \times 2\pi$. From the SEM images (Fig. 1c–f and Fig. 2a₃–c₃), all the shells with different average shell thicknesses (9–32 nm) could not withstand the imbalance induced by the resultant forces, i.e., osmotic pressure (P) and centrifugal force (F_c), and then one part of the shell caved in toward the opposite side to form hollow bowl-shaped HOPBs-BINOL with circular opening, symmetrical wall and hemi-spherical profile. As shown in TEM images (Fig. 3), the bright

regions at the bottom of HOPBs-BINOL, emblazoned with an arrow, represented voids between two semi-shells and the dark regions were the particle shells, which stated clearly that a part of the shells caved in to enclose a void inside HOPBs-BINOL with a kippah structure.

3.2. Characterization of HOPBs-TRIP

In view of thin shell thickness in favor of mass transfer of reactants and high content of (*R*)-6 beneficial to form more TRIP, the hollow bowl-like HOPBs-BINOL with an average shell thickness of 18 nm was selected as a precursor to prepare supported chiral phosphoric acid HOPBs-TRIP by the reaction of phenolic hydroxyl groups in HOPBs-BINOL with POCl₃ and then hydrolysis of phosphoryl chloride (Scheme 1). From the SEM (Fig. 4b) and TEM (Fig. 4c) images, the as-prepared HOPBs-TRIP remained the similar hollow bowl-like shape as its own precursor HOPBs-BINOL. From FT-IR spectra, the successful phosphorylation of phenolic hydroxyl groups to form phosphoric acid $(-O)_2P(=O)OH$ was qualitatively confirmed by the emerging stretching vibration absorption of P=O bond at 1531 cm⁻¹ and the disappeared stretching vibration, in-plane flexural vibration and out-plane flexural vibration of phenolic O–H bond at 3512 cm⁻¹, 1374 cm⁻¹ and 650 cm⁻¹ (Fig. 4a). Furthermore, the quantitative functionalization level of phenolic hydroxyl groups in HOPBs-BINOL to form phosphoric acid by phosphorylation and hydrolysis was determined to be 0.15 mmol g⁻¹ by elemental analysis of P content. In particular, the disappeared IR absorption peak of water in HOPBs-BINOL at 1677 cm⁻¹ was attributed to the dehydration of adsorbed water in the presence of POCl₃.

3.3. Screening of reaction conditions

Given the versatility of chiral homoallylic alcohols as building blocks in synthesis and the simplicity of reaction protocol [47–52], the asymmetric allylboration of aromatic aldehydes was selected as a model reaction to investigate the catalytic performance of hollow bowl-like HOPBs-TRIP. From Table 1, it was found that HOPBs-TRIP (5 mol%) promoted the asymmetric allylboration of benzaldehyde with allylboronic pinacol ester in toluene at 25 °C to afford allylic alcohol **3a** in 96% yield with 90% ee (Entry 1). When the reaction temperature decreased from 25 °C to –30 °C, the enantioselectivities were significantly improved to 96% ee in constant yields (entry 2, 3). Although the reaction gave the excellent yield (96%) and enantioselectivity (95% ee) at 0 °C in the first run, the enantioselectivity in recycled runs at 0 °C descended quicker than that at –30 °C. To maintain the high excellent enantioselectivity, the low temperature (–30 °C) was selected as a suitable parameter to carry out the following reactions. Further lowering the used amount of HOPBs-TRIP to 1 mol% allowed the reaction to reach the similar yield (95%) but low enantioselectivity (90% ee, entry 5), whereas no further significantly improved yield and % ee were achieved upon increasing the dosage of HOPBs-TRIP to 10 mol% (entry 4). Solvent played an important role in the catalytic performances. In other solvents such as EtOAc and CH₂Cl₂, HOPBs-TRIP promoted the reaction in lower yields with poorer enantioselectivities (entries 7, 9). Even worse: no product was obtained in THF (entry 9), which elucidated that the catalytic performances of the heterogeneous nano-bowls were closely related with solvent properties. It was ever-reported that the reaction proceeded via a transition state involving both a hydrogen-bonding interaction from the catalyst hydroxyl group to the pseudoaxial oxygen of cyclic boronate and a stabilizing interaction from the phosphoryl oxygen of TRIP to the formyl hydrogen of the aldehyde [53]. Then, it was conjectured that the formation of hydrogen bond between oxygen atoms in EtOAc and THF and hydroxyl group of TRIP interfered with the hydrogen-bonding interaction of the hydroxyl group in TRIP with the oxygen of cyclic boronate, and ultimately resulted in the decreased yields of products or even inactive allylboration.

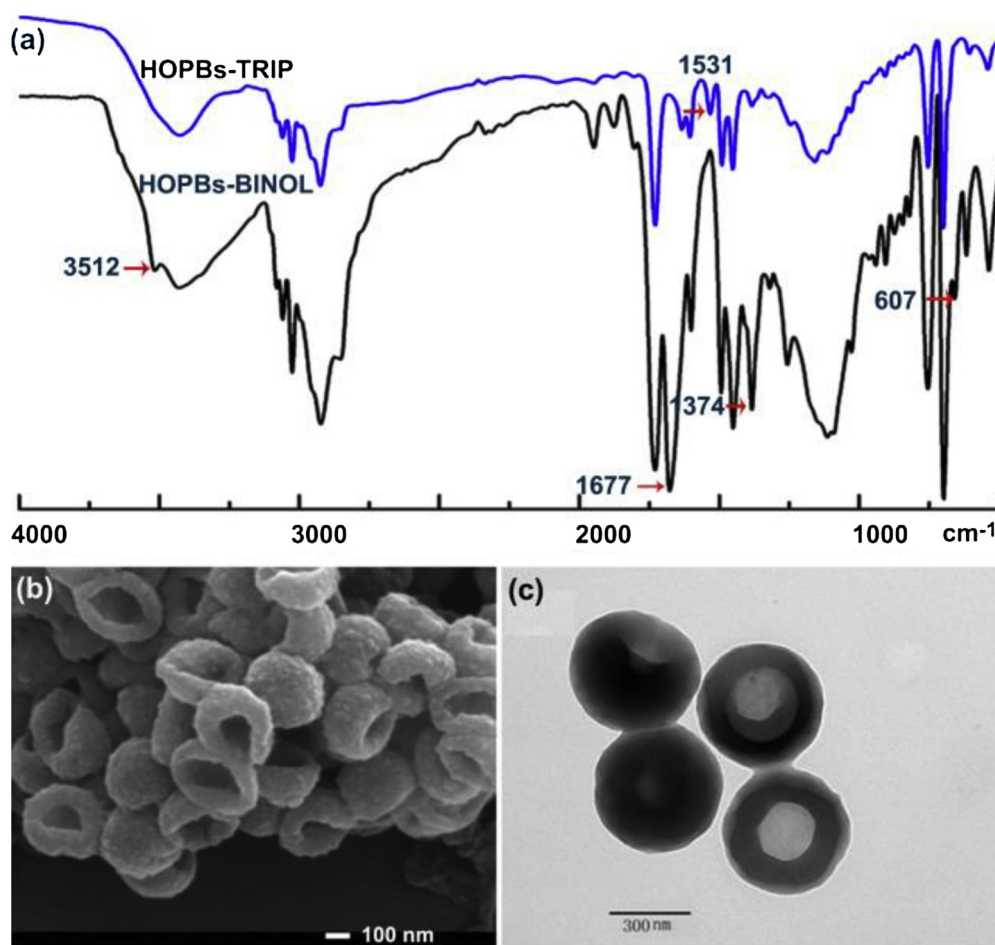


Fig. 4. IR spectra (a) of HOPBs-BINOL and HOPBs-TRIP, SEM (b) and TEM(c) images of hollow bowl-like HOPBs-TRIP.

Table 1

Screening of catalytic reaction conditions of HOPBs-TRIP in the asymmetric allylboration of benzaldehyde with allylboronic pinacol ester.^a

	Solvent	Cat. (mg/mol%)	T (°C)	t (h)	Yield (%) ^b	Ee (%) ^c
1	Toluene	66.7/5	25	6	96	90
2	Toluene	66.7/5	0	6	96	95
3	Toluene	66.7/5	-30	6	95	96
4	Toluene	133.4/10	-30	6	96	96
5	Toluene	13.3/1	-30	6	95	90
6	Toluene	66.7/5	-30	16	96	97
7	EtOAc	66.7/5	-30	6	65	48
8	THF	66.7/5	-30	6	traces	n.d.
9 ^f	CH ₂ Cl ₂	66.7/5	-30	6	90	80

^a Reactions carried out in 1.0 mL of solvent, benzaldehyde (21.2 mg, 0.2 mmol) and allyl boronic acid pinacol ester (36.9 mg, 0.22 mmol).

^b Isolated yields.

^c Determined by chiral HPLC on Daicel Chiralpak OD-H column.

3.4. Enhanced catalytic activity of hollow bowl-like HOPBs-TRIP

To elucidate the morphology-dependent catalytic activity of HOPBs-TRIP, the contrast PS-TRIP with a diameter of 3–5 μm and no hollow structure (Fig. S3) was prepared according to the ever-reported procedure [36]. In the asymmetric allylboration of 4-chlorobenzaldehyde with allylboronic pinacol ester under the fine-tuned conditions (5 mol % TRIP, 0.2 mol L⁻¹ in toluene, -30 °C, 6 h), the concentrations of 4-chlorobenzaldehyde and the yields of corresponding product (*R*)-1-(4-chlorophenyl)but-3-en-1-ol, plotted versus reaction time during the whole reaction, were obtained by HPLC and shown in Fig. 5. It was

found that the concentrations of 4-chlorobenzaldehyde and yields of (*R*)-1-(4-chlorophenyl)but-3-en-1-ol displayed the different reaction kinetics for HOPBs-TRIP and PS-TRIP. Hollow bowl-like HOPBs-TRIP exhibited the higher catalytic activities than PS-TRIP in the whole process, which was attributed to the shorter seepage distance and internal and external concentration difference of reactants for HOPBs-TRIP. The reaction kinetics of 4-chlorobenzaldehyde, promoted by HOPBs-TRIP, followed a linear Eq. (3) in the whole reaction with a high degree of fitting ($R^2 = 0.981$). However, in PS-TRIP-promoted allylboration, the concentrations of 4-chlorobenzaldehyde versus reaction time could be expressed by an exponential function (Eq. (4)) during the first 3 h and then a linear Eq. (5), respectively with the high degrees of fitting ($R^2 = 0.990$ and 0.960).

$$\text{HOPBs-TRIP: } c_1 = -0.031t + 0.188, R^2 = 0.981 \quad (3)$$

$$\text{PS-TRIP: } c_2 = 0.06 \exp(-t/0.598) + 0.140, R^2 = 0.990 \text{ (0–3 h)} \quad (4)$$

$$c_3 = -0.034t + 0.221, R^2 = 0.960 \text{ (3–6 h)} \quad (5)$$

Then, differentiating the concentration (c) with respect to time (t), the reaction rates of 4-chlorobenzaldehyde at time (t) were expressed by the following equation.

$$\text{HOPBs-TRIP: } d[c_1]/dt = -0.031 \quad (6)$$

$$\text{PS-TRIP: } d[c_2]/dt = -0.1003 \exp(-t/0.6028) + 7.534e-5 \text{ (0–3 h)} \quad (7)$$

$$d[c_3]/dt = -0.034 \text{ (3–6 h)} \quad (8)$$

The initial reaction rates at 1 h are calculated to be 0.031 mol L⁻¹ h⁻¹ and 0.019 mol L⁻¹ h⁻¹, respectively for HOPBs-TRIP and PS-TRIP. At the beginning of the reaction, the reaction rate mainly

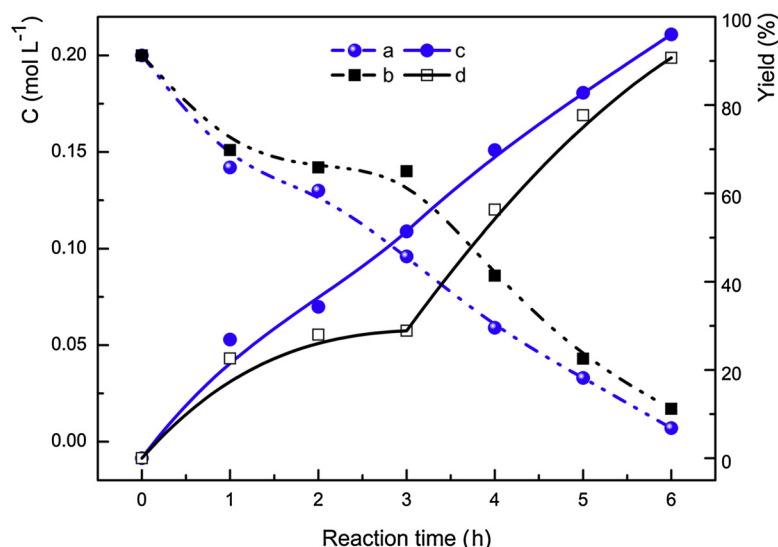


Fig. 5. Concentrations of 4-chlorobenzaldehyde (a: HOPBs-TRIP, b: PS-TRIP) and yields of (*R*)-1-(4-chlorophenyl)but-3-en-1-ol (c: HOPBs-TRIP, d: PS-TRIP) versus reaction time in the allylboration of 4-chlorobenzaldehyde with allylboronic pinacol ester.

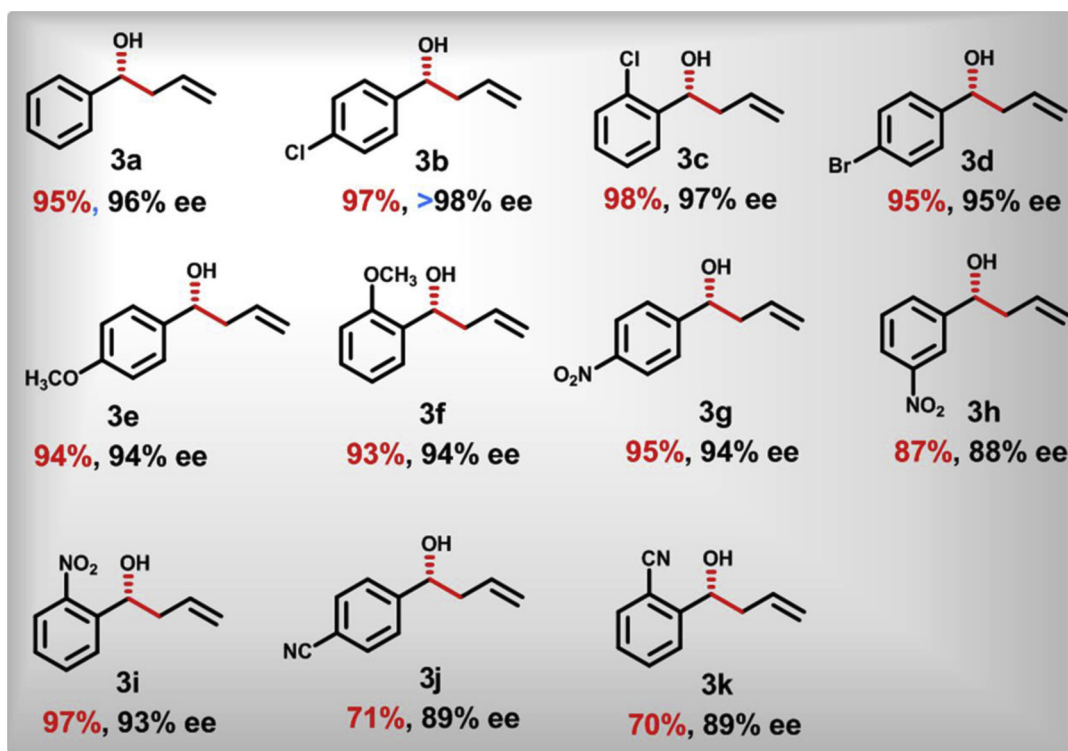


Fig. 6. Yields and enantioselectivities of homoallylic alcohol products in the heterogeneous asymmetric allylboration of aromatic aldehydes with allylboronic pinacol ester promoted by hollow bowl-like HOPBs-TRIP.

depended on surface reaction. Owing to the larger surface area ($17.6 \text{ m}^2 \text{ g}^{-1}$) of HOPBs-TRIP than that of PS-TRIP ($2.1 \text{ m}^2 \text{ g}^{-1}$), the higher catalytic rate of HOPBs-TRIP was observed. As the reaction progressed, HOPBs-TRIP possessed the constant catalytic rate and PS-TRIP showed a sharply decreased catalytic rate ($6.8 \times 10^{-4} \text{ mol L}^{-1} \text{ h}^{-1}$) at 3 h. At this point, the gap in catalytic rate between HOPBs-TRIP and PS-TRIP reached the maximum, which was likely involved in the slower molecule diffusion in the inner of PS-TRIP resulted from the longer seepage distance and the lack of internal/external concentration difference of reactants. After 4 h, the reaction rate of PS-TRIP was enhanced to a constant value ($0.034 \text{ mol L}^{-1} \text{ h}^{-1}$) owing to the establishment of internal molecular diffusion equilibrium in the inner of PS-

TRIP. Based on the above-mentioned catalytic reaction kinetics and enhanced catalytic activity of HOPBs-TRIP, it was concluded that the short seepage distance and hollow structure, obtained by the controllable fabrication of hollow nano-bowl with a thin shell thickness, were favorable for the fast mass transfer of reactants to access the catalytic sites and improved the effectiveness factor (η) of supported heterogeneous TRIP [43,54].

3.5. Scope of aromatic aldehydes promoted by hollow bowl-like HOPBs-TRIP

Encouraged by the enhanced catalytic activity of hollow bowl-like

HOPBs-TRIP in the asymmetric allylboration of 4-chlorobenzaldehyde with allylboronic pinacol ester, the scope was extended to various aromatic aldehydes under the optimal conditions: 5 mol % TRIP, 0.2 mol L⁻¹ of aromatic aldehydes in toluene (1 mL), -30 °C, 6 h). From Fig. 6, HOPBs-TRIP proved to be an effective heterogeneous chiral phosphoric acid in the synthesis of highly enantioenriched homoallylic alcohols. It was found that the electron-poor and electron-rich aromatic aldehydes were generally well-tolerated to afford the products **3a** – **k** in moderate to high yields (70–98%) with good to excellent enantioselectivities (88–98% ee). More importantly, most of the products gave the higher enantioselectivities, compared with the ever-reported results [36]. Especially, different from the ever-reported moderate enantioselectivity of *ortho*-chlorinated derivative (72% ee), HOPBs-TRIP promote the allylboration of *ortho*-substituted aromatic aldehydes to afford the corresponding derivatives (**3c**, **3f** and **3i**) in high yields (93–98%) with excellent enantioselectivities (92–98% ee). Unfortunately, (*R*)-4-(1-Hydroxybut-3-en-1-yl)benzotrile (**3j**) and (*R*)-2-(1-Hydroxybut-3-en-1-yl)benzotrile (**3k**) seemed to be the exception, giving the lower yield (70%) with a poorer enantioselectivity (88% ee). The reason for this decreased activity of HOPBs-TRIP was possibly attributed to the interaction of basic cyano (-CN) group with the phosphoric acid in HOPBs-TRIP.

3.6. Reusability and comprehensive evaluation of hollow bowl-like HOPBs-TRIP

After the completion of the allylboration reaction, HOPBs-TRIP could be simply recovered by centrifugal separation and directly reused in the following catalytic cycles. It was found that the remained yield (95%) of (*R*)-1-Phenylbut-3-en-1-ol (**3a**) with a slightly lowered enantioselectivity (94% ee) was achieved in the sixth run. To remain an excellent enantioselectivity (> 95% ee), the 6th-reused HOPBs-TRIP was dispersed in 5 mL of DI water and adjusted to pH = 1–2 by HCl (1 mol L⁻¹). The recovered HOPBs-TRIP regained the same excellent catalytic performances (95%, 96% ee) as its fresh HOPBs-TRIP, and could further catalyze another six cycles in high yields (92–95%) with excellent enantioselectivities (94–96% ee) in an accumulated TONs of 226 (Table S2). The outstanding stability of HOPBs-TRIP was further confirmed by no significant loss of phosphorus in elemental analysis (0.14 mmol g⁻¹) and no obvious change in morphology from its SEM image (Fig. S5).

Although the total yield (12%) of chiral monomer (*R*)-**6** starting from (*R*)-BINOL via six steps was much lower than that (22%) of homogeneous TRIP via four steps, HOPBs-TRIP afforded the higher accumulated TONs of 226 in > 92% yield with > 95% ee than homogeneous TRIP with the TONs of 20 in 99% yield with 98% ee [48], which was attributed to the disposable use of homogeneous TRIP and calculated after a total of 12 cycles of catalyst reuse (Table S2). From a TOF's point of view, there was still a big gap in TOF between heterogeneous HOPBs-TRIP (3.2 h⁻¹) and homogeneous TRIP (19.8 h⁻¹) in the asymmetric allylboration of benzaldehyde. Moreover, HOPBs-TRIP with a thin shell thickness (18 nm) and hollow structure possessed the faster initial catalytic reaction rate (0.031 mol L⁻¹ h⁻¹) than ever-reported heterogeneous PS-TRIP (0.019 mol L⁻¹ h⁻¹). Therefore, based on the resource utilization of TRIP, the as-fabricated hollow bowl-like HOPBs-TRIP could be considered to be more effective than heterogeneous PS-TRIP and homogeneous TRIP in the asymmetric allylboration of benzaldehydes with allylboronic pinacol ester.

4. Conclusions

The enhancement of mass transfer of reactants to active catalytic sites has always been one of the most consistently pursued research topics in the field of heterogeneous catalysis. In this paper, to take advantage of the merits of the short seepage distance and hollow structure in favor of mass transfer in heterogeneous catalysis, hollow

organic polymeric nano-bowls-supported BINOL-derived chiral phosphoric acid (HOPBs-TRIP) was fabricated for the first time via the copolymerization of functional monomers on the surface of poly(styrene/acrylic acid) nanospheres (PS), etching of PS by DMF and functionalization by POCl₃. Owing to the thin shell thickness and hollow structure, the as-fabricated hollow bowl-like HOPBs-TRIP displayed the higher catalytic activity and enantioselectivities than ever-reported PS-TRIP in the allylboration of aromatic aldehydes, and showed outstanding stability in bowl-like morphology and good reusability in catalytic performance (92% and 94% ee in the twelfth cycle) with an accumulated TONs as high as 226. It is believed that HOPBs-TRIP has great attraction for the large-scale synthesis and the heterogenization of other successful homogeneous catalysis, especially for mass transfer-limited multi-component reactions.

Acknowledgement

This work was supported by Basic Science and Advanced Technology Research Project of Chongqing Science & Technology commission (cstc 2017jcyjBX0027).

Appendix A. Supplementary data

Supplementary material related to this article can be found, in the online version, at doi:<https://doi.org/10.1016/j.mcat.2018.12.014>.

References

- [1] B. Pugin, H.U. Blaser, *Top. Catal.* 53 (2010) 953–962.
- [2] S. Itsuno, M.M. Hassan, *RSC Adv.* 4 (2014) 52023–52043.
- [3] D.B. Zhao, K.L. Ding, *ACS Catal.* 3 (2013) 928–944.
- [4] S.W. Cao, F.L. Tao, Y. Tang, Y.T. Li, J.G. Yu, *Chem. Soc. Rev.* 45 (2016) 4747–4765.
- [5] Y. Li, W.J. Shen, *Chem. Soc. Rev.* 43 (2014) 1543–1574.
- [6] F. Teng, G.X. Xie, L. Zhang, X.B. Ma, *ChemCatChem* 10 (2018) 4586–4593.
- [7] S. Hoffmann, A.M. Seayad, B. List, *Angew. Chem., Int. Ed.* 44 (2005) 7424–7427.
- [8] F. Auria-Luna, E. Marques-Lopez, R.P. Herrera, *Adv. Synth. Catal.* 359 (2017) 2161–2175.
- [9] S.K. Nimmagadda, S.C. Mallojjala, L. Woztas, S.E. Wheeler, J.C. Antilla, *Angew. Chem. Int. Ed.* 56 (2017) 2454–2458.
- [10] Z.M. Liu, H. Zhao, M.Q. Li, Y.B. Lan, Q.B. Yao, J.C. Tao, X.W. Wang, *Adv. Synth. Catal.* 354 (2012) 1012–1022.
- [11] F.E. Held, D. Grau, S.B. Tsogoeva, *Molecules* 20 (2015) 16103–16126.
- [12] A. Zamfir, S. Schenker, M. Freund, S.B. Tsogoeva, *Org. Biomol. Chem.* 8 (2010) 5262–5276.
- [13] S. Hoffmann, A.M. Seayad, B. List, *Angew. Chem., Int. Ed.* 44 (2005) 7424–7427.
- [14] M. Rueping, A.P. Antonchick, T. Theissmann, *Angew. Chem., Int. Ed.* 45 (2006) 3683–3686.
- [15] M. Rueping, A.P. Antonchick, *Angew. Chem., Int. Ed.* 46 (2007) 4562–4565.
- [16] J.P. Reid, J.M. Goodman, *Org. Biomol. Chem.* 15 (2017) 6943–6947.
- [17] J.G. de Vries, N. Mrcic, *Catal. Sci. Technol.* 1 (2011) 727–735.
- [18] Z.H. Zhang, W.S. Sun, G.M. Zhu, J.X. Yang, M. Zhang, L. Hong, R. Wang, *Chem. Commun. (Camb.)* 52 (2016) 1377–1380.
- [19] K. Bera, C. Schneider, *Org. Lett.* 18 (2016) 5660–5663.
- [20] K. Bera, C. Schneider, *Chem. Eur. J.* 22 (2016) 7074–7078.
- [21] Y. Zhang, Y.F. Ao, Z.T. Huang, D.X. Wang, M.X. Wang, J.P. Zhu, *Angew. Chem., Int. Ed.* 55 (2016) 5282–5285.
- [22] J. Calleja, A.B. Gonzalez-Perez, A.R. de Lera, R. Alvarez, F.J. Fananas, F. Rodriguez, *Chem. Sci.* 5 (2014) 996–1007.
- [23] Y.M. Deng, S. Kumar, K. Wheeler, H. Wang, *Chem. Eur. J.* 21 (2015) 7874–7880.
- [24] H. Wu, Q. Wang, J.P. Zhu, *Angew. Chem., Int. Ed.* 55 (2016) 15411–15414.
- [25] H. Wu, Q. Wang, J.P. Zhu, *Angew. Chem., Int. Ed.* 56 (2017) 5858–5861.
- [26] F.T. Zhou, H. Yamamoto, *Angew. Chem., Int. Ed.* 55 (2016) 8970–8974.
- [27] M. Biedrzycki, A. Kasztelan, P. Kwiatkowski, *ChemCatChem* 9 (2017) 2453–2456.
- [28] S.K. Nimmagadda, S.C. Mallojjala, L. Woztas, S.E. Wheeler, J.C. Antilla, *Angew. Chem., Int. Ed.* 56 (2017) 2454–2458.
- [29] J.P. Reid, J.M. Goodman, *Chem. Eur. J.* 23 (2017) 14248–14260.
- [30] Z. Yan, X. Gao, Y.G. Zhou, *Chin. J. Catal.* 38 (2017) 784–792.
- [31] L.M. Overvoorde, M.N. Grayson, Y. Luo, J.M. Goodman, *J. Org. Chem.* 80 (2015) 2634–2640.
- [32] C. Lalli, P. van de Weghe, *Chem. Commun. (Camb.)* 50 (2014) 7495–7498.
- [33] L.M. Overvoorde, M.N. Grayson, Y. Luo, J.M. Goodman, *J. Org. Chem.* 80 (2015) 2634–2640.
- [34] D.S. Kundu, J. Schmidt, C. Bleschke, A. Thomas, S. Blechert, *Angew. Chem., Int. Ed.* 51 (2012) 5456–5459.
- [35] B.H. Zhang, L.X. Shi, R.X. Guo, *Catal. Lett.* 145 (2015) 1718–1723.
- [36] L. Clot-Almenara, C. Rodríguez-Escrich, L. Osorio-Planes, M.A. Pericàs, *ACS Catal.* 6 (2016) 7647–7651.

- [37] L. Clot-Almenara, C. Rodríguez-Esrich, M.A. Pericàs, RSC Adv. 8 (2018) 6910–6914.
- [38] X. Zhang, A. Kormos, J. Zhang, Org. Lett. 19 (2017) 6072–6075.
- [39] X.J. Wang, J. Feng, Y.C. Bai, Q. Zhang, Y.L. Yin, Chem. Rev. 116 (2016) 10983–11060.
- [40] A.M. El-Toni, M.A. Habila, J.P. Labis, Z.A. AlOthman, M. Alhoshan, A.A. Elzatahry, F. Zhang, Nanoscale 8 (2016) 2510–2531.
- [41] J.H. Ko, N. Kang, N. Park, H.W. Shin, S. Kang, S.M. Lee, H.J. Kim, T.K. Ahn, S.U. Son, ACS Macro Lett. 4 (2015) 669–672.
- [42] Z.W. Zhao, D.D. Feng, G.X. Xie, X.B. Ma, J. Catal. 359 (2018) 36–45.
- [43] F.Q. Dai, Z.W. Zhao, G.X. Xie, D.D. Feng, X.B. Ma, ChemCatChem 9 (2017) 89–93.
- [44] A. Modak, A. Bhaumik, Chemistryselect 1 (2016) 1192–1200.
- [45] J.H. Xu, J. Pang, D.D. Feng, X.B. Ma, Mol. Catal. 443 (2017) 139–147.
- [46] D. Cheng, S. Wang, J.A.M. Kuipers, Chem. Eng. Sci. 160 (2017) 80–84.
- [47] Z.P. Lu, M.M. Dias, J.C.B. Lopes, G. Carta, A.E. Rodrigues, Ind. Eng. Chem. Res. 32 (1993) 1839–1853.
- [48] P. Jain, J.C. Antilla, J. Am. Chem. Soc. 132 (2010) 11884–11886.
- [49] P. Jain, H. Wang, K.N. Houk, J.C. Antilla, Angew. Chem., Int. Ed. 51 (2012) 1391–1394.
- [50] M. Chen, W.R. Roush, J. Am. Chem. Soc. 134 (2012) 10947–10952.
- [51] C.A. Incerti-Pradillos, M.A. Kabeshov, A.V. Malkov, Angew. Chem., Int. Ed. 52 (2013) 5338–5341.
- [52] E. Rodríguez, M.N. Grayson, A. Asensio, P. Barrio, K.N. Houk, S. Fustero, ACS Catal. 6 (2016) 2506–2514.
- [53] M.N. Grayson, S.C. Pellegrinet, J.M. Goodman, J. Am. Chem. Soc. 134 (2012) 2716–2722.
- [54] G.X. Xie, J.K. Tian, S. Wei, X.Z. Liu, X.B. Ma, Appl. Catal. A Gen. 565 (2018) 87–97.